Response to review by Anonymous Referee #1

We thank the reviewer for the constructive comments made to our manuscript 'Climate controls on water vapor deuterium excess in the marine boundary layer of the North Atlantic based on 500 days of in situ, continuous measurements"

The reviewer points out that we spend a significant portion of the manuscript on describing out setup and protocols. We do not completely agree that the 'Material and method' section is too long (the review claims that we spend 70% on the technical method – The material and Method section is 7 pages of text while the manuscript is 17 pages, but we do have 8 out 12 figures dealing with characterization of the system). We strongly believe that it is very important to robustly characterize these relative novel measurements types. For example we find it very important to point out that despite the fact that these type of instruments perform measurements with ~1 second resolution it does not make sense of claiming this high resolution due to memory effects in the inlet lines. While some instruments, which we have worked with have shown significantly less drift than this instrument, it is clear that it is very important to document and correct the drift.

We have below answered the explicit comments using green text

1.P2377 L.7 and other part "d-excess vs wind-speed relationship" Diffusional 18-O fractionation factor dependency on wind speed was investigated using 17O-excess data (Uemura et al. 2010). The observed diffusional fractionation factors are scattered and do not show clear dependency on wind speed (Fig 2 in their paper). On the contrary recent study showed that d-excess dependency on surface wind speed (Benetti et al., 2014). This discussion paper supports the former. The inconsistency is even confusing because the first author of this discussion paper is a coauthor of Benetti et al. (2014). I guess that the wind dependency differ widely depending on sampling location/height, moisture source and weather conditions etc. The authors should clarify the differences and discuss possible reasons.

References: Ryu Uemura, Eugeni Barkan, Osamu Abe, and Boaz Luz, Triple isotope composition of oxygen in atmospheric water vapor, Geophysical Research Letters, VOL. 37, L04402, doi:10.1029/2009GL041960, 2010

Marion Benetti, Gilles Reverdin, Catherine Pierre, Liliane Merlivat, Camille Ris, Hans Christian Steen-Larsen, Françoise Vimeux, Deuterium excess in marine wa- ter vapor: Dependency on relative humidity and surface wind speed during evap- oration, Journal of Geophysical Research, Volume 119, Issue 2, 584–593, 2014 DOI:10.1002/2013JD020535

We agree with the reviewer that these presented data does not give much support to the theory of MJ79. However we want to point out that we do not state that the definition by MJ79 or the results of Uemuerra et al 2010 or Benetti et al. 2014 is wrong. We simply state that the data collected in Bermuda does not give find support for the effect of wind

speed by MJ79. Specifically do we write in the text:

"

This indicates that either the wind regimes defined in MJ79 might not be appropriate for this area or the observed d-excess of the local water vapor is affected by past wind conditions.

"

We acknowledge the need to clarify that we do not state that an effect of wind speed cannot be observed other places. Hence we introduce the following sentence in the text in end of the section dealing with wind speed.

The differences between the result of this study and the results by Uemura et al. (2012) and Benetti et al. (2014) illustrates that more studies are needed to clarify the effect of wind speed on the d-excess signal in the marine boundary condition.

Technical corrections:

P2366, L21-22 ". . .which alter the slope of 8 due to temperature dependence of theequilibrium fractionation coefficient. . ..."C443

The slope is changed any process that does not follow the D/18O slope of 8 (i.e., not only the temperature). Indeed the crude approximation of logarithm $(1+\delta)$ is an important artifacts (Appendix in Uemura et al., 2012).

References: Uemura, R., V. Masson-Delmotte, J. Jouzel, A. Landais, H. Motoyama, and B. Stenni, Ranges of moisture-source temperature estimated from Antarctic ice cores stable isotope records over glacial–interglacial cycles, Clim. Past, 8, 1109-1125, 2012, doi:10.5194/cp-8-1109-2012

Yes – this is indeed correct. The approximation of the logarithm definition is indeed a reason why the slope decreases significantly at depleted values similar to those found in Antarctica. However the values of change in d18O we are encountering here is between -8 and -16 o/oo. In a log dD vs. log d18O plot the slope of the meteoric waterline for this region will vary between approximately 9 and 9.3.

We do acknowledge that the text is not completely correct and have corrected it such that it does not give the impression that any equilibrium process will lead to a slope of 8.

P2368, L19 "water vapor isotope system" >water vapor isotope monitoring system

Corrected

P2370, L13, "..and provides the measurement, which are the focus of this paper". What

does this sentence mean? All the data (fig 10 to 13) are from this top inlet?

Yes that is correct. We use only measurements from the top inlet in the paper.

P2373, L21-21, "We first injected air with two significantly different water vapor concen- trations.. and secondly injected . . ..with two significantly different water vapor isotopic compositions". It is difficult to make such water vapors. How did you prepare the different vapor? Please describe in detail.

It is correct that if only the SDM Picarro module was available this would indeed be difficult. However since our self-designed calibration system was build to generate a constant stream of vapor we simply replicated this system and used it to generate the water vapor injected at the inlet.

We follow the advise of the reviewer and add the following sentence to the text

"We used a similar system as our calibration system described in section 2.2 to generate the water vapor with the given isotope and humidity value."

P2374, L24, ". . ..a second Picarro inc. analyzer " Add product name (2120-i or 2130-i)?

This was a special test version Picarro inc. analyzer and did therefore not have a specific number. I presume it was with the similar specs as 2130-i.

P2375, L3, ". . ..The mean he mean deviation for " > Remove "he mean".
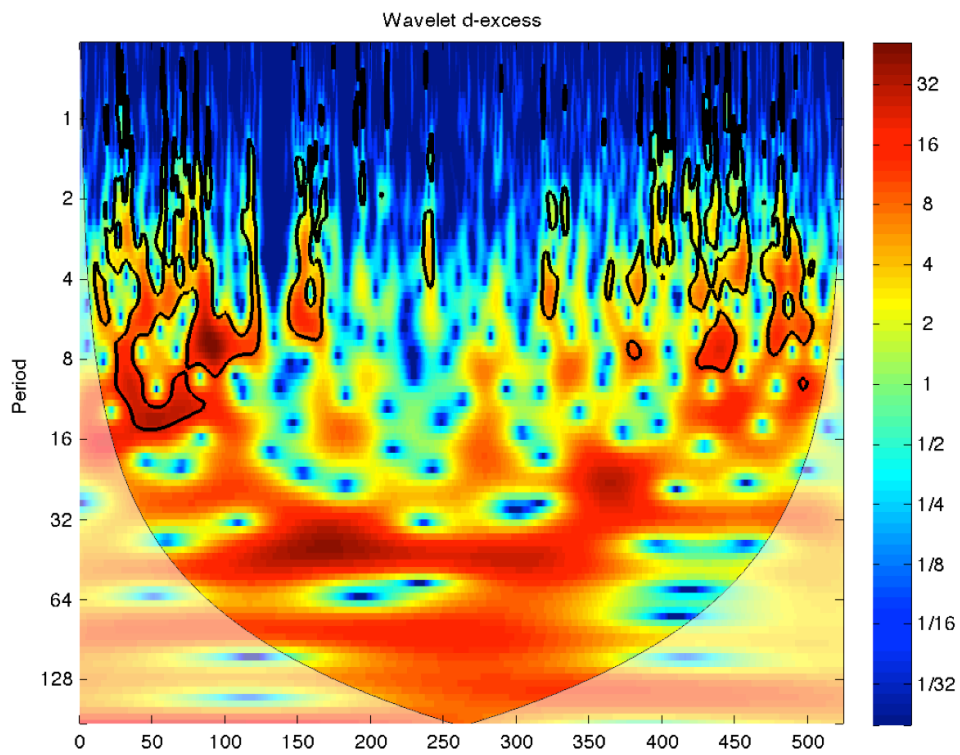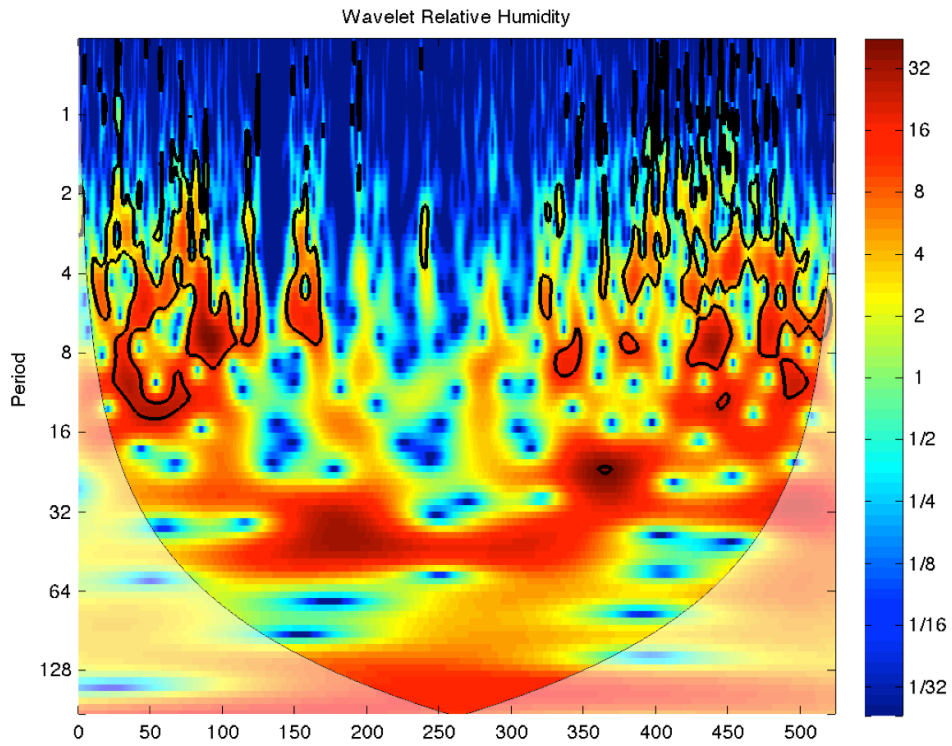
Corrected

P2378, L20, ". . ..This is supported by a wavelet analysis showing significant. . . " Where is the figure showing the wavelet analysis?

To limit the numbers of figures we choice not to show the figure. The wavelet analysis is shown below:

P2379, L16, ". . ..allows for ntegration. . .. . " >integration

Corrected

Wavelet Relative Humidity

Wavelet d-excess

Response to review by Anonymous Referee #2

We thank the reviewer for the detailed and helpful comments made to our manuscript 'Climate controls on water vapor deuterium excess in the marine boundary layer of the North Atlantic based on 500 days of in situ, continuous measurements"

We notice that Reviewer # 2 has raised concerns with our conclusion regarding the finding that the wind speed does not affect the observed d-excess. We agree in general with the reviewer that this is an important finding, but we do not agree that we make a strong conclusion based on this finding. Instead we merely report our findings and show that they cannot be used to support the predicted relationship between d-excess and wind speed given by MJ79:

Below we list the sentences from the manuscript, which deals with this finding. We do not find that these sentences constitute strong conclusions.

However, in contrast with theory, no effect of wind speed could be detected on the relationship between *d*-excess and relative humidity.

This indicates that either the wind regimes defined in MJ79 might not be appropriate for this area or the observed *d*-excess of the local water vapor is affected by past wind conditions.

However, we could not identify any shifts in relationship with wind speed.

We have below commented on the individual concerns by Reviewer #2 using green text.

General remarks: The scientific investigation is focused on the relationship between deuterium excess and relative humidity, based on the model assumptions of Merlivat and Jouzel (1979). It is certainly good to test the MJ model assumptions and results us- ing this new data set. However, the paper would profit from a discussion of the model assumptions. In particular, I think here of the threshold in wind speed for "smooth" and "rough" conditions (corresponding to up to 4Bft below and larger than 5Bft above the threshold, thus not that different) and also of the assumption that the vapour is produced locally. The influence of waves on surface roughness and on potential evap- oration area is not discussed either. From Fig. 1 it is obvious that 5-10 m/s is the most frequent wind speed, which means that most of your measurements are in the upper range of "smooth conditions" and the lower range of "rough conditions". I would not expect to find a large difference for those two regimes. It is a too strong conclusion that the wind speed has no influence on the deuterium excess or the d-humidity relation- ship. It would be better to really compare the low and high end of the wind speed range to get a clearer picture.

The reason that we choose to separate the wind speed for a smooth regime define for wind speed < 6 m/s and a rough regime defined for wind speed > 7 m/s is due to discontinuity in the 'k'-factor (MJ79) giving rise to differences in kinetic fractionation (Figure 2 – MJ79 – inserted below)

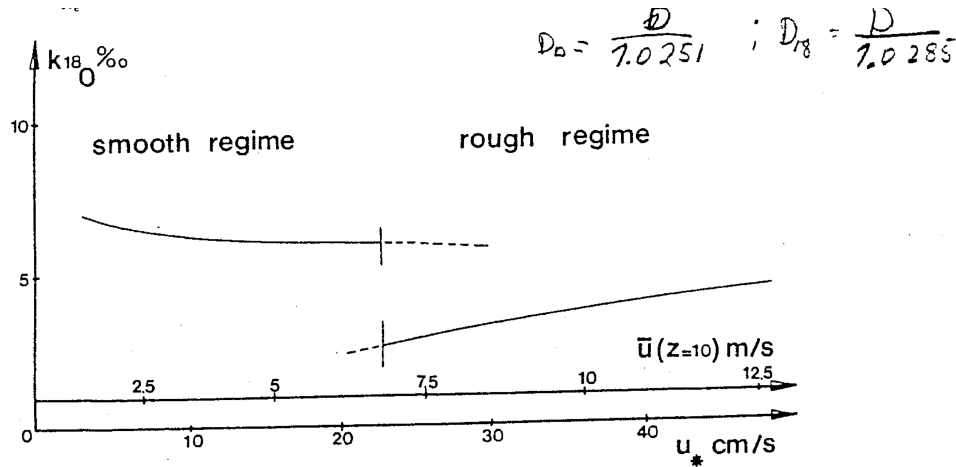$$D_o = \frac{D}{1.0251} \quad ; \quad D_{18} = \frac{D}{1.0285}$$

Fig. 2. Variation of the kinetic fractionation factor for oxygen 18, k_{18}, with the friction velocity or the mean wind speed at $z = 10$ m.

In this figure it can be clearly seen that the discontinuity arises between 6 and 7 m/s – hence why we make this separation.

We have, in order to illustrate the finding that our data does not support the theory related to effect of wind speed on the d-excess, separated the observations into 4 different wind speed regions: below 3 m/s, between 3 and 5 m/s, between 7 and 9 m/s and above 9 m/s. The result of this is shown in the figures below. We believe that these figures also support our finding that observations from Bermuda is not in agreement with the theory related to wind speed of MJ79. We want to highlight that we do not state that MJ79 is wrong but just that data collected from Bermuda is not consistent with the theory of MJ79. There can be several reasons for this.

We notice that for wind speeds above 9 m/s we see for RH<0.5 a slightly lower d-excess values compared to wind speeds below 3 m/s. This is of course consistent with theory of MJ79 but the magnitude is not as large. We would expect a difference in d-excess according to MJ79 of about 10 o/oo (we might observe a slight decrease of about 2-3 o/oo but only for RH<0.5). We notice that evaporation of sea spray droplets would indeed have a similar effect as we would include water vapor of same isotopic composition as the ocean.
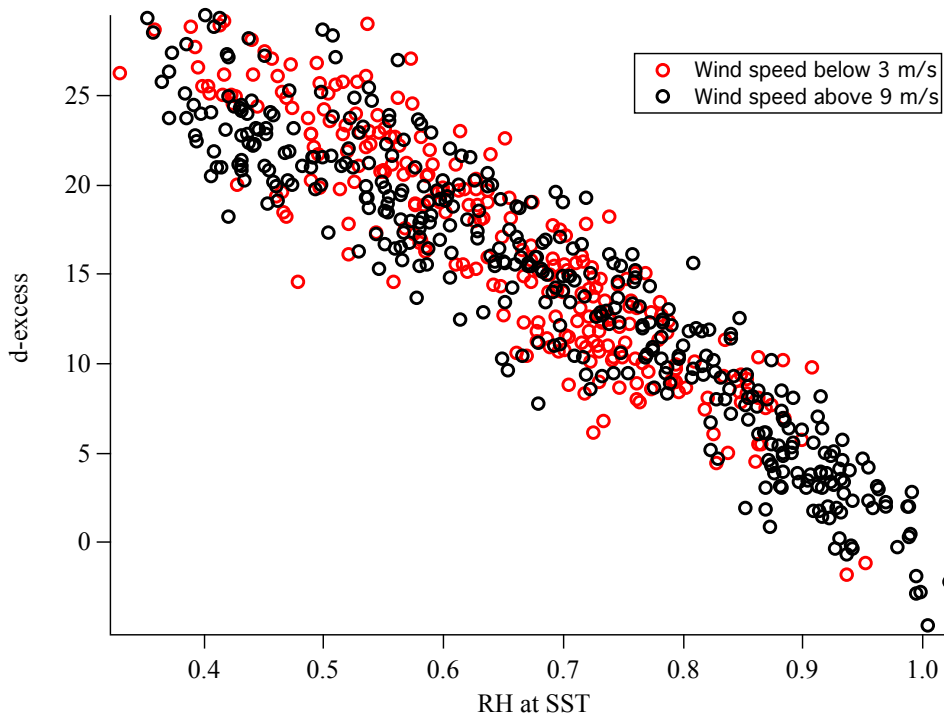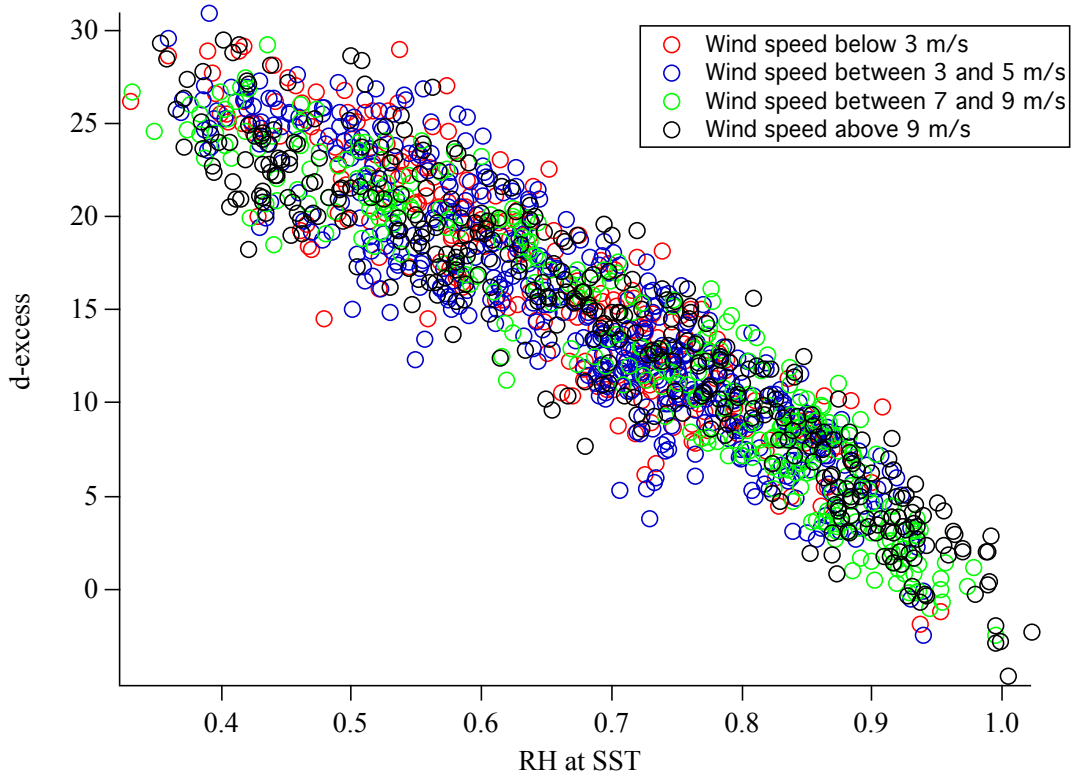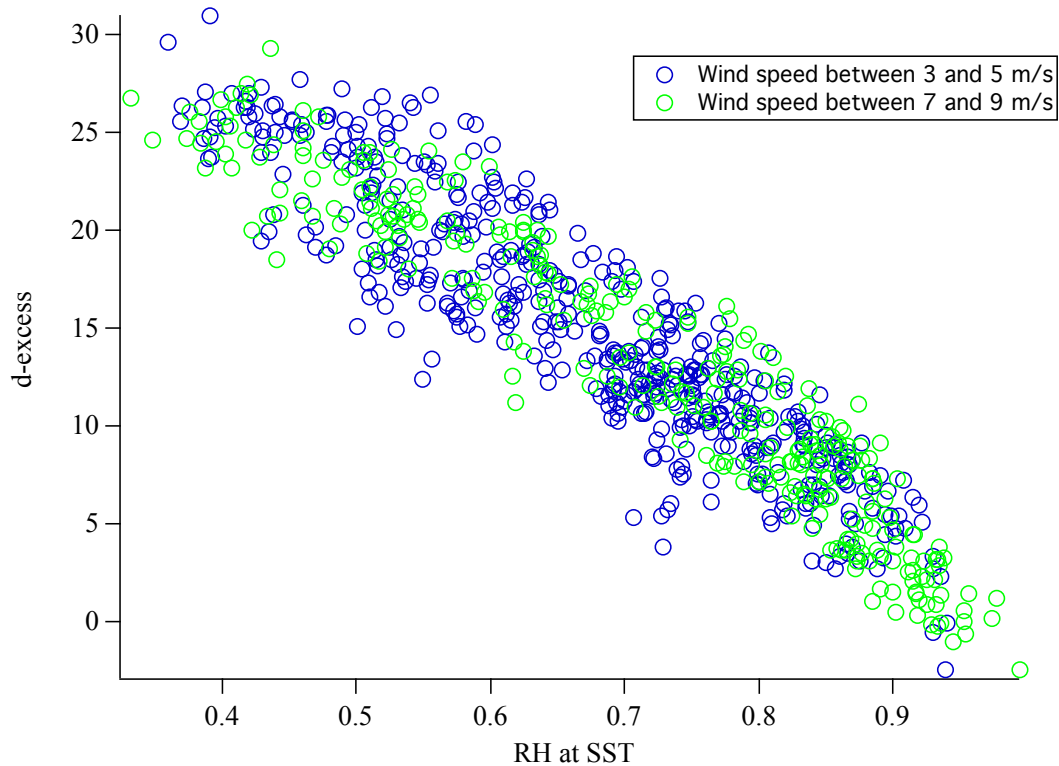
Also, the question of local or non-local origin of the moisture is only briefly discussed. Low wind-speed could also be associated with high-pressure and thus more local origin of the moisture, whereas higher wind speeds might mean advection of moisture. The differences in the results for different wind directions also hint at some influence here. These points should be addressed more clearly.

Yes we completely agree on this point. We have therefore updated the sentence to read:

"

… the observed d-excess of the local water vapor is affected by past wind conditions at remote areas of evaporation
"

Specific remarks: In atmospheric science, humidity is commonly defined as relative, absolute or specific humidity or as mixing ratio. Another measure is humidity ppmv, but this can refer to dry air or to humid air (mostly it refers to dry air, but it is not clearly defined). You can choose the humidity measure you like, of course, but, for the above mentioned reasons, it would be good if you could define the humidity measure you use in

your study.

We acknowledge this issue and have inserted the following equation defining our humidity measure:

"

Humidity (ppmv) = $p_w/(p_{tot}-p_w) 10^6$, where p_w and p_{tot} is the vapor pressure and the total pressure.

"

"Relative humidity normalized to SST" is an expression that is not only confusing but incorrect. Relative humidity is always given AT a certain temperature. What you use is the relative humidity at SST, but it is not a normalized value.

Yes – we acknowledge that our choice of words were not optimal. We have corrected this through out the paper and in the figures.

Technical remarks:

Check the use of "respectively", in most cases it is used incorrectly

Corrected

P2367: l22: but the strong correlation. . .

Corrected

L23: do you mean "not allow identifying the impact of rhSST alone?

No we meant

"not allow identifying the independent impact of SST."

We have corrected this.

P2375, l11: better: at the beginning of autumn

Corrected

L16: parallel to

Corrected

L23: do you mean "without any significant local effect"?

Yes - Corrected

P2376/fig. 10: the x-axis should be months not tenth of a year, that is hard to read, and in the text you refer to months, too.

L22: here you refer to <6m/s and~10m/s, later you compare <6 and >7m/s. ??

Corrected to the following text:

and a~rough surface (wind speed above 7\,\unit{m\,s^{-1}} – kinetic fractionation value take for 10\,\unit{m\,s^{-1}})

P2377: l25: approximately rather than around

Corrected

P2378, L1: lower winter SST (not colder)

Corrected

L7: moisture back trajectory calculations is not a good expression. You have quite a few VERY long words that should at least contain a dash (-) at the right position.

Corrected

L25: prevents frontal systems from passing through

Corrected

P2379: l6: signal-to-noise ratio

Corrected

L15: increasing the average time from 2 weeks to 1 month does not significantly further accept this slope.

Corrected

L16/17: This sentence is not understandable, please reformulate

Yes we absolutely agree – sorry. This has been corrected now.

"

We note that time averaging allows for integration across synoptic systems. This is comparable to a spatial averaging across air masses in the region around the Bermuda Islands.

"

L19: become closer

Corrected

L23: reflectSpeculation is not a very scientific method, better use hypothesis

Corrected

P2380: l11: coming from the American continent (or do you mean off?)

Yes – we meant 'off'. This is corrected now.

P2381: l2: suggesting a limited. . .

Corrected

Response to review by Anonymous Referee #3

We thank the reviewer many times for the comments made to our manuscript 'Climate controls on water vapor deuterium excess in the marine boundary layer of the North Atlantic based on 500 days of in situ, continuous measurements"

Yes we do agree with the reviewer that part of the 'Materials and method' has been introduced in our previous manuscript 'Continuous monitoring of summer surface water vapor isotopic composition above the Greenland Ice Sheet'. However we do not think it will be possible to shorten the section as the analysis in the rest of the manuscript depends on the individual subsections. Particularly, section 2.4 and 2.5 is of very great importance as this part support the robustness of the measurements. Section 2.3 deals with the drift and as this system does show a quite significant drift compared to other systems. It is important for us to argue why this is indeed a correct and how we adjust for this.

We have in the answered the individual comments below using green text

Specific comments,

P2367, 20-25, missing date during "Gat et al., Pfahl and Wernli, and Uemura et al.".
corrected

p2368, 5, "with the availability of ......provided..... Tremoy et al., 2012).", there is no subject for "provided"
corrected

P2369, 15-20, "Monthly mean sea surface temperatures" should be "Monsthly mean SST".
corrected

P2369, 20-25, I think the part of "Other measurements carried out at the tower consist of sampling for the Global Atmosphere Passive Sampler Network, continuous lower atmosphere ozone measurements and discrete greenhouse gas sampling for NOAA's Earth System Research Laboratory, continuous measurements of aerosol optical depth for NOAA's Aerosol Robotic Network, and continuous solar radiation measurements for NOAA's Baseline Surface Radiation Network." has no connection with this paper, so it should be deleted.
It is correct that the other measurements presented here are not directly related to the presented analysis. However we would prefer to keep this section as this paper is also meant to present the setup, data collection routine and outline future study directions.

P2377, 20-25, the definition of summer and winter is cited from any paper or is defined by the authors? Why use this definition?

We acknowledge that this definition is subjective. As argued in Merlivat and Jouzel 1979 the d-excess in the evaporated vapor depends on the SST. We therefore define a cold period (winter for SST < 21C) and a warm period (summer for SST > 26C). We wanted to separate the SST as much as possible but also wanted a sufficiently large enough dataset. Hence why we chose this definition.

Fig.11. It's easy to understand the figure if the fit lines use the same color with the dots.
We have tried to change the colors of the linear regression fits but did not get a better/easier way to illustrate the variability.

```
\documentclass[acpd, online, hvmath]{copernicus_discussions}

\begin{document}\hack{\sloppy}

\title{Climatic controls on water vapor deuterium excess in the marine boundary
layer of the North Atlantic based on 500 days of in situ, continuous
measurements}

\Author[1,2]{H.~C.}{Steen-Larsen}
\Author[3]{A.~E.}{Sveinbj\"{o}rnsdottir}
\Author[4]{A.~J.}{Peters}
\Author[1]{V.}{Masson-Delmotte}
\Author[4]{M.~P.}{Guishard}
\Author[5]{G.}{Hsiao}
\Author[1]{J.}{Jouzel}
\Author[2]{D.}{Noone}
\Author[4]{J.~K.}{Warren}
\Author[6]{J.~W.~C.}{White}

\affil[1]{Laboratoire des Sciences du Climat et de l'Environnement, UMR CEA-
CNRS-UVSQ/IPSL 8212, Gif-sur-Yvette, France}
\affil[2]{Department of Atmospheric and Oceanic Sciences, and Cooperative
Institute for Research in Environmental Sciences, University of Colorado,
Boulder, Colorado, USA}
\affil[3]{Institute of Earth Sciences, University of Iceland, Reykjavik,
Iceland}
\affil[4]{Bermuda Institute of Ocean Sciences, St. George's GE 01, Bermuda}
\affil[5]{Picarro Inc., Santa Clara, California, USA}
\affil[6]{Institute of Arctic and Alpine Research, Campus Box 450, University of
Colorado, Boulder, Colorado, USA}


\correspondence{H.~C.~Steen-Larsen (hanschr@gfy.ku.dk)}

\runningtitle{Climatic controls on water vapor deuterium excess}
\runningauthor{H.-C.~Steen-Larsen et~al.}


\received{6~December~2013}
\accepted{20~January~2014}
\published{}


\firstpage{1}

\maketitle


\begin{abstract}
  Continuous, in situ measurements of water vapor isotopic composition
  have been conducted in the North Atlantic, Bermuda Islands
  (32.26$^\circ$\,N, 64.88$^\circ$\,W) between November 2011 and
  June~2013, using a~cavity-ring-down-spectrometer water vapor isotope
  analyzer and an autonomous self-designed calibration
  system. Meticulous calibration allows us to reach an accuracy and
```

precision on 10\,min average of δ^{18}O, δ{D}, and
d-excess of 0.14\,\permil, 0.85\,\permil, and
1.1\,\permil, verified using two parallel instruments with
independent calibration. As a~result of more than 500 days with
6\,hourly data the relationships between deuterium excess, relative
humidity (rh), sea surface temperature (SST), wind speed and
direction are assessed. From the whole dataset, 84\,\% of
d-excess variance is explained by a~strong linear relationship
with relative humidity. The slope of this relationship ($-
$42.6\,$\pm$\,0.4\,\permil~\% (rh)) is similar to the theoretical
prediction of Merlivat and Jouzel (1979) for SST between
20\,$^\circ$C and 30\,$^\circ$C. However, in contrast with theory,
no effect of wind speed could be detected on the relationship
between d-excess and relative humidity. Separating the dataset
into winter, spring, summer, and autumn seasons reveals different
linear relationships between d-excess and humidity. Changes in
wind directions are observed to affect the relationships between
d-excess and humidity. The observed seasonal variability in the
relationship between d-excess and relative humidity underlines
the importance of long-term monitoring to make accurate conclusions.
\end{abstract}

\introduction

Water stable isotopes in the atmosphere are key tracers of physical processes
within the hydrological cycle. Since the 1950s, water stable isotopes of
precipitation and their imprint in many different natural archives have been
measured by mass spectrometry and understood in relation to processes
controlling evaporation and evapotranspiration, moisture transport and
condensation (Epstein and Mayeda, 1953; Dansgaard, 1954; Rozanski et~al.,
1993). The founding works of Dansgaard (1964) and Craig and Gordon (1965)
have shaped the last ~ 50\,\unit{yr} of research using water isotopes.
The knowledge of hydrological cycle processes is fundamental for the
implementation of water stable isotopes in conceptual Rayleigh distillation
models or atmospheric regional or general circulation models, and their
various applications such as the quantitative interpretation of ice core
records (Johnsen et~al., 1989; Jouzel et~al., 1997). Here, we will focus on
the basis of the atmospheric water cycle: the relation between
\chem{H_2^{18}O} and HD\chem{^{16}O} compared to \chem{H_2^{16}O} in the
marine boundary layer near the ocean surface. We will use the delta-notation
introduced by Craig (1961a):
\begin{align}
\nonumber
  &
\delta^{\ast} =
\left(\frac{R_{\text{sample}}}{R_{\text{VSMOW}}}-1\right) \times 1000,
\end{align}
where $\delta^\ast$ represents either \chem{\delta^{18}O} or $\delta
D$, and R_{sample} and R_{VSMOW} is the
isotopic ratio of the sample and the Vienna Standard Mean Ocean Water.

As noted by Craig (1961b), the relationship between \chem{\delta^{18}O} and
δD reflects the imprint of kinetic and equilibrium fractionation
processes. The second order parameter d-excess has been defined by

Dansgaard (1964) in order to highlight the isotopic variability, which is not
driven by equilibrium fractionation that otherwise for the isotopic values
encountered here leads to a~linear
relationship between \chem{\delta^{18}O} and δD with a~global mean
slope of 8 ({\permil}/{\permil}) (Majoube, 1971):
\begin{align}
\nonumber
d\,{\text{-excess}} = \delta D - 8 \times \chem{\delta^{18}O}
\end{align}

Without large changes in temperature along the distillation path (which alter
the slope of 8 due to the
temperature-dependence of the equilibrium fractionation coefficients),
changes in d-excess are dominated by kinetic fractionation. As
qualitatively explained by e.g. Dansgaard (1964), the kinetic effect during
evaporation arises from the different diffusivities of the water isotopes
\chem{H_2^{16}O}, HD\chem{^{16}O}, and \chem{H_2^{18}O} in the air. This
kinetic fractionation during evaporation was formally described by Merlivat
and Jouzel (1979) (hereafter MJ79) under an idealized ``closure assumption''
implying no advection of moisture. They formulated theoretical relationships
between d-excess, sea surface temperature (SST) and relative humidity of
the air compared to the saturation vapor pressure at the ocean surface
(rhSST). We will in the following refer to rhSST as relative humidity
at the SST. The relationships were expected to depend on the wind
regime affecting molecular and turbulence mixing at the ocean surface,
following the evaporation theory of Brutsaert (1975). Assessing the validity
of MJ79 calculations requires long-term monitoring of water vapor isotopes in
the marine boundary layer in order to separate the effect of the different
influencing factors.

During the past decades only a~few observations of surface water vapor
isotopes have been conducted in the marine boundary layer due to the
analytical challenges associated with cryogenic sampling. Gat et~al.~(2003)
conducted cryogenic sampling of water vapor in the eastern Mediterranean and
reported high d-excess values, due to strong kinetic effect produced as dry
air transported from Europe moved across the warm Mediterranean Sea,
a~finding further supported by the study of Pfahl and Wernli (2009).
Similarly, in another study, high d-excess values measured in several
Arctic areas were attributed to high kinetic effect produced by dry polar air
at the sea ice margin (Kurita, 2011; Steen-Larsen et~al., 2013). Uemura
et~al.~(2008) cryogenically collected 60 samples of water vapor onboard
a~research vessel during a~one-month crossing of the Southern Ocean from
Australia to Antarctica and back to South Africa. Consistent with the theory
of MJ79, a~strong relationship was observed between d-excess and rhSST
(with a~slope of $-58\,{\permil} per {\%}} rhSST), but the strong correlation
between rhSST and SST did not allow identifying the independent impact of SST.
Pfahl and Sodemann (2013) used data from Gat et~al.~(2003), Pfahl and Wernli
(2009), and Uemura et~al. ~(2008) to propose a~globally applicable
interpretation of d-excess
in precipitation based on the overall linear relationship between surface
vapour d-excess and rh. A~recent support for the strong relationship
between d-excess in the marine boundary layer water vapor and rh was
obtained from a~one-month campaign in the eastern North Atlantic by Benetti
et~al.~(2014) (slope of $-45\,{\permil} per {\%}} rhSST). The difference
between findings from Uemura et~al.~(2008) and Benetti et~al.~(2014) open

Hans Christian Steen…, 4/15/14 10:15 AM
Deleted: normalized to

Hans Christian Steen…, 4/15/14 10:43 AM
Deleted: a~

Hans Christian Steen…, 4/15/14 10:43 AM
Deleted: alone

Hans Christian Steen-…, 4/14/14 2:15 PM
Deleted: .

Hans Christian Steen-…, 4/14/14 2:15 PM
Deleted: ~

Hans Christian Steen…, 4/15/14 11:39 AM
Deleted: n

Hans Christian Steen…, 4/15/14 11:40 AM
Deleted: n

questions about both temporal and spatial variability in the relationship between d-excess and rh.

With the availability of commercial laser water vapor isotope analyzers (Crosson et~al., 2002; Baer et~al., 2002), it has recently become possible to perform accurate and continuous in situ measurements if correct protocols are implemented for the calibration of the measurements. Further developments have allowed the setup of autonomous systems in remote field sites in regions spanning from Greenland to Niger, producing records of the variability of surface water vapor isotopic composition over seasons to years (e.g. Steen-Larsen et~al., 2013; Bonne et~al.,~2013; Tremoy et~al.,~2012). With the goal of performing year-round measurements of water vapor isotopic composition in the North Atlantic marine boundary layer, we have focused on the Bermuda Islands. The location was chosen due to warm SST as a~result of the nearby Gulf Stream current, and because this area is expected to be a~key moisture source for the North Atlantic sector. Indeed, part of our motivation was to characterize the isotopic composition at the source of moisture for Greenland and therefore to improve the understanding of the processes governing Greenland water stable isotopes and the interpretation of d-excess from Greenland ice core records (e.g. Steen-Larsen et~al., 2011; Johnsen et~al., 1989; Fisher, 1992; Masson-Delmotte et~al., 2005; Jouzel et~al.,~2007). For this purpose, we have designed a~water vapor isotope monitoring system with the goal of being completely autonomous for periods of several months and able to perform frequent drift-calibrations in order to have high accuracy for the d-excess. Section~2 presents the setup of this system and our protocol for calibration of our measurements. Using two water vapor isotope analyzers calibrated independently of each other allows us to estimate the accuracy and precision of our observations. Section~3 is devoted to the investigation of statistical relationships and drivers for the observed variability in the d-excess: seasonality, wind direction, and wind speed as well as effect of averaging over different number of days.

\section{Materials and method}

\subsection{Meteorological observations}

As shown in Fig.~1, our water vapor isotope monitoring system was installed at the Tudor Hill Atmospheric Observatory in Bermuda (32.26°\,N 64.88°\,W). Air temperature and relative humidity (rh) were recorded using a~Campbell Scientific CR1000 logger (±0.1\,{\degree}C and ±2\,{\%} rh) and wind direction and speed using a~RM Young propeller-type vane ($\pm3{\degree}$ and ±0.3\,\unit{m\,s^{-1}}). Distribution of wind direction and speed is shown in Fig.~1d indicating that the wind is predominantly straight in from the ocean (~ 65\,{\%} occurrence). Surface pressure data values are obtained from the meteorological observations taken by the Bermuda Weather Service at Bermuda's L. F. Wade International Airport nearby. During the few days when we had meteorological data gaps at Tudor Hill, we used the airport observations by the Bermuda Weather Service. Monthly sea surface temperature data (SST) was obtained by averaging daily MODIS-aqua satellite observations over a~~ 600\,\unit{km}\,$\times$\,800\,\unit{km} area centered on Bermuda (Haines et~al., 2007; Acker and Leptoukh, 2007). Mean monthly air temperature data ranges from 17.7\,{\degree}C (February, mean daily high/low: 19.8\,{\degree}C/15.5\,{\degree}C) to 27.2\,{\degree}C (August, mean daily

high/low: 29.8\,{\degree}C/24.5\,{\degree}C). Monthly mean SST vary from
18.4\,{\degree}C to 28.2\,{\degree}C (minimum/maximum:
March/August). Monthly climatology data 1949--1999 (Air temperature and SST)
were obtained from the Bermuda Weather Service. Other measurements carried
out at the tower consist of sampling for the Global Atmosphere Passive
Sampler Network, continuous lower atmosphere ozone measurements and discrete
greenhouse gas sampling for NOAA's Earth System Research Laboratory,
continuous measurements of aerosol optical depth for NOAA's Aerosol Robotic
Network, and continuous solar radiation measurements for NOAA's Baseline
Surface Radiation Network.

\subsection{Setup}

We installed in November~2011 a~water vapor isotope analyzer from Picarro
inc. (Model {\#} HBDS-2120) at the Tudor Hill Atmospheric Observatory in
Bermuda, where the base of the meteorological tower is at $\sim
29$\,\unit{m}\,a.s.l. (meters above sea leve) and situated $\sim
30$\,\unit{m} from the coast. The instrument is installed inside
a~temperature regulated box ensuring daily temperature variability $<
0.2$\,{\degree}C, which itself is placed inside an air-conditioned container
where diurnal temperature variability is < 2\,{\degree}C. The setup of the
system (Fig.~1c) is similar to the setup previously deployed above the
Greenland ice sheet (Steen-Larsen et~al., 2013). Three inlets were initially
installed on the tower at a~height of ~ 20.5\,\unit{m} above ground
(~ 49\,\unit{m}\,a.s.l.), ~ 13.1\,\unit{m} above ground ($\sim
42$\,\unit{m}\,a.s.l.), ~ 5.8\,\unit{m} above ground ($\sim
35$\,\unit{m}\,a.s.l.). In June~2013 we installed a~separate fourth inlet
~ 2.5\,\unit{m}\,a.s.l. The top inlet placed ~ 49\,\unit{m}\,a.s.l.
is well above local vegetation (scrub) and provides the measurements, which
are the focus of this paper.

Air sampling is performed using copper tubing, as laboratory
experiments showed copper to cause less smoothing of the signal
compared to for example stainless steel and PTFE. All inlet tubes were
placed inside Armaflex{$^{\text{\textregistered}}$} closed cell tube
insulation and heated to above 50\,{\degree}C using self-regulating
heat trace from Raychem{$^{\text{\textregistered}}$}. To prevent rain
from being sucked into our air sampling tubes, the entrance of the
inlets was placed inside Nalgene{$^{\text{\textregistered}}$} bottles
with their bottoms removed and substituted by a~wire mesh screen to
prevent intrusion of foreign objects, such as insects. An extra shield
was placed above the inlets for protection against frequent intense
precipitation events. A~10\,\unit{L\,min^{-1}} air pump ensures a~quick
transport of the air from the start of the inlet and into the
analyzer. An extra 5\,\unit{L\,min^{-1}} air pump maintains a~constant
flow in the tubes not being sampled. Inside the temperature-regulated
box, a~manifold operated by the analyzer controls which inlet is being
measured. A~three-way valve controls whether the analyzer measures
ambient water vapor, or water vapor from the calibration unit. The
purpose of the calibration unit is to supply the analyzer with water
vapor of known isotopic composition. This is achieved by using
a~similar vapor source as described by Elleh{\o}j et~al.~(2013). Dry
air is let to slowly bubble through water of known isotopic
composition kept at constant temperature inside a~glass bottle (5\,L).
Elleh{\o}j et~al.~(2013) showed that the water vapor isotopes

Hans Christian Steen-…, 4/14/14 2:18 PM
Deleted: sea surface . … [1]

are stable over flow rates up to 150\,\unit{mL\,min^{-1}}, which is well
above the flow rates used here (~ 30\,\unit{mL\,min^{-1}}). As the
temperature of the system is very stable, the known isotopic
composition and temperature of the water are used to calculate the
isotopic composition of the generated water vapor under the assumption
of isotopic equilibrium. This saturated water vapor is instantly
diluted with dry air (humidity level below 200\,\unit{ppmv} generated
from Drierite{$^{\text{\textregistered}}$}) as it leaves the glass
bottle to prevent any condensation in the tubes and thereby isotopic
fractionation. We used this vapor generation system to perform
humidity-isotope response calibrations and for drift corrections, as
introduced in Steen-Larsen et~al.~(2013) and described hereafter.

\subsection{Calibration}

As described in Steen-Larsen et~al.~(2013) it is necessary to perform
a~humidity-isotope response calibration of the analyzer, and correct
the raw measurements. Following the protocol described in Steen-Larsen
et~al.~(2013), water vapor with a~constant isotopic composition is
introduced into the instrument at different humidity levels, obtained
by diluting the saturated water vapor coming out of our
bubbler-system. We vary the humidity in steps of 10\,min, but start
and finish the sequence at the same humidity level in order to correct
for drift of the system. The drift is assumed to be linear between the
start and stop of each sequence. To assess the stability of the
humidity-isotope response through time, calibrations were repeated at
different dates (Fig.~2). Small but significant drifts in the
humidity-isotope response curve are observed over the monitoring
period. To correct for this observed drift of the humidity-isotope
response, we assume the drift to be linear between two consecutive
humidity-isotope response calibrations.

To reference our measurements against the international IAEA
VSMOW-SLAP scale, we measured standards of known isotopic
composition. Between 3 and 10 different standards, which varied
between ~ 0 and $\sim {-}39$\,{\permil} in \chem{\delta^{18}O} and
between ~ 0 and $-$310\,{\permil} in δD, were used each
time we carried out a~VSMOW-SLAP calibration. The standards used were
referenced by respectively the Institute of Arctic and Alpine Research
at University of Colorado, Centre for Ice and Climate at University of
Copenhagen, and Laboratoire des Sciences du Climat et de
l'Environnement in Gif-sur-Yvette, and calibrated against the IAEA
VSMOW-SLAP. The standard deviation of the residuals between the
VSMOW-SLAP value of the standards and the calculated values based on
best linear fits is ~ 0.1\,{\permil} for \chem{\delta^{18}O} and
~ 1.1\,{\permil} for δD. We carried out VSMOW-SLAP
calibrations in November~2011, August/September~2012 (most intensive
period of calibrations, with 6 calibrations within 3 weeks), and
June~2013 (Table~1). Table~1 rules out short-term variability for the
VSMOW-SLAP slope but shows long-term changes in the slope, similar to
values reported by Bastrikov et~al.~(2014). We assume that the
VSMOW-SLAP slope varies linearly between the calibration periods. This
observed drift is small, and has no impact on our data quality. The
range of observed atmospheric water vapor isotope variability is less
than ~ 10\,{\permil} in \chem{\delta^{18}O}, and much smaller

than the range of the standards. An un-accounted drift of 0.01 in the
VSMOW-SLAP \chem{\delta^{18}O} slope would for example result in
a~maximum bias of only 0.1\,{\permil} in \chem{\delta^{18}O} of the
measured atmospheric water vapor isotope signal.

To account for the drift of the measured atmospheric water vapor
isotope signal, we measure every 6--12\,h water vapor with a~known
isotopic composition. This is carried out using our bubbler system
described above. We have monitored the isotopic composition of the
water inside our bubbler by taking samples regularly for measurements
on an IRMS-system. As expected from the minor removal of water vapor
(~ 0.03\,\unit{g}/drift calibration) and large water body (5\,L), no change
in the liquid water isotopic composition was
detected. The water vapor from the bubbler is measured for 30\,min of
which the first 15\,min are discarded due to memory effects. The raw
measurements are corrected using our humidity-isotope response
correction (Fig.~2). They are then calibrated against VSMOW-SLAP using
the slopes presented in Table~1 and drift corrected using the
measurements of the vapor from the bubbler and the expected isotopic
composition of the water vapor calculated from the equilibrium
fractionation coefficient and the liquid water isotope value.

Figure~3 shows the long-term drift of the system, characterized
for \chem{\delta^{18}O} and δD by a~~ 3\,{\permil} increase and
a~~ 7\,{\permil} decrease over the ~ 1.5\,\unit{yr} measurement
period. The associated ~ 25\,{\permil} drift of d-excess stresses the
uttermost importance of this correction. No apparent reason for this drift
could be determined. The stable isotopic measurements of water samples taken
from the bubbler rule out a~drift of the standard itself. We note a~long-term
correlation between the drift and the temperature of the calibration system
and analyzer (Fig.~3). However, abrupt changes in the temperature do not seem
to induce any response of the system. A~48\,h running mean (black line,
Fig.~3) is used to drift correct the measurements of the atmospheric water
vapor isotopes.

The Picarro humidity measurements are calibrated against the estimated
absolute humidity (ppmv) from the Campbell humidity sensor showing
a~strong linear relationship (Fig.~4). Humidity (ppmv) = $p_w/(p_{tot}-p_w)$
10^6, where p_w and p_{tot} is the vapor pressure and the total pressure.
Hereafter, we use the corrected Picarro humidity values.

\subsection{Signal smoothing due to the experimental setup}

Due to the length of the introduction line (25\,\unit{m} of tubing), we
expect the signal to be smoothed through mixing and interactions with the
inside tube wall (Massman and Ibrom, 2008). By using a~10\,\unit{L\,min^{-1}}
pump to transport the sample quickly from the inlet to the analyzer we try to
minimize the smoothing of the signal from the interactions between the water
vapor and the walls of the tubing. In order to quantify this effect, two sets
of experiments were performed. We first injected air with two significantly
different water vapor concentrations (~ 1000\,\unit{ppmv} and $\sim
30$\,000\,\unit{ppmv}) and secondly injected air containing the same
concentration of water vapor, but with two significantly different water
vapor isotopic compositions (\chem{\delta^{18}O}: ~-56\,{\permil} and

$\sim -$17\,{\permil}$). We used a similar system as our calibration system described in section 2.2 to generate the water vapor with the given isotope and humidity value. The observed step changes in the humidity and isotope values are shown in Fig.~5. The normalized response functions for the shifts in humidity, \chem{\delta^{18}O}, and δD together with the averaged time derivative of the normalized response functions are shown in Fig.~6. A~log-normal distribution gives a~good fit (not shown) to the time derived normalized response functions. The lag time for the signal to arrive at the analyzer (defined as the time at which 0.5\,{\%} of the normalized response has been reached) is shorter for the humidity (~ 40\,s) than for the isotopes (~ 50\,s). Similarly, 95\,{\%} of the normalized response is obtained after respectively ~ 225\,s, ~ 650\,s, and ~ 1200\,s for the humidity, \chem{\delta^{18}O}, and δD signal. This smoothing of the signal between the inlet and the analyzer causes different memory effects on each parameter. Since the performed step changes can be approximated by a~Heaviside step function for the humidity and isotopic change, the first time-derivative of the original humidity and isotope signal becomes a~Dirac delta function. The transfer function (i.e. the dampening of the signal at different frequencies) of the complete set-up can therefore be estimated from the Fourier transform of the time derivative of the normalized change. This is shown in Fig.~7 for humidity (black lines), \chem{\delta^{18}O} (blue lines), and δD (red lines). A~signal with a~periodicity of ~ 100\,s will be attenuated by ~ 85\,{\%} in humidity, 98.5\,{\%} in \chem{\delta^{18}O}, and 99.7\,{\%} in δD. However, it is potentially possible to record humidity signals with a~periodicity down to ~ 30\,s. Due to a~compensation between larger smoothing and lower noise level for δD (compared to \chem{\delta^{18}O}), it is possible to observe signals in both δD and \chem{\delta^{18}O} with a~periodicity down to ~ 60\,s. Using the estimated transfer function for δD and \chem{\delta^{18}O} and the fact that the measured signal is equal to the original signal convoluted by a~log-normal function, it could be possible to perform a~back-smoothing correction and recreate the original high frequency signal using similar techniques as applied to ice core water stable isotope records or eddy-covariance analysis (Johnsen, 1977; Johnsen et~al., 2000; Spank and Bernhofer, 2008).

\subsection{Instrumental inter-comparison and inter-site variability}

During autumn 2012, a~second Picarro inc. analyzer was installed in parallel with the original analyzer for a~short period of time. Each analyzer was calibrated independently using the above procedure. The comparison of the two records allows us to directly estimate the uncertainty of the measured water vapor isotope signal, including the uncertainty of each of the calibration steps. Based on 10\,min averaged calibrated data from the two analyzers, spanning a~period of 5 days (Fig.~8), the inter-instrument differences are normally distributed with a~mean and standard deviation of 0.05\,$\pm$\,0.14\,{\permil} (\chem{\delta^{18}O}), $-$0.15\,$\pm$\,0.85\,{\permil} (δD), and 0.3\,$\pm$\,1.1\,{\permil} (d-excess). The mean deviation for \chem{\delta^{18}O}, δD, and d-excess being close to zero rules out any systematic bias between the two analyzers. Following Steen-Larsen et~al.~(2013), the standard deviation of the inter-instrument differences is used as a~conservative estimate for our precision. Our obtained precision of 1.1\,{\permil} for d-excess far exceeds the precision of water vapor cryogenic trapping capabilities and

reaches the precision achieved by IRMS.

In order to investigate the regional coherency of the observed water
vapor isotopes, we have implemented the second analyzer at the
opposite end of the Bermuda Islands, located 20\,\unit{km} away from
Tudor Hill observatory (Fig.~1) for a~period of ~ 3 days
t the beginning of autumn (Julian day 249--252 of 2012). The comparison of
the two records (Fig.~9) depicts a~gradient in humidity levels,
probably due to the altitude at which measurements were conducted
(~ 15\,\unit{m}\,a.s.l vs. ~ 49\,\unit{m}\,a.s.l. for Tudor
Hill). Altogether, a~very good agreement is observed between
observations at either end of the island. During an event at which the
wind blew parallel to with the axis formed by the two stations, at day
251.1, we observe a~1\,h delay between the first increase of humidity
and water vapor isotopic composition at the northern site (Fig.~9,
black solid line), and the same signals recorded at Tudor Hill
(20\,\unit{km} away). This is fully consistent with air mass
transportation at the mean wind speed of about 20\,\unit{km\,h^{-1}}
without any significant difference in the magnitude of the water vapor
isotopic signal between the two sites. Based on this short comparison,
we conclude that the signal measured at Tudor Hill is representative
of a~regional signal, without any significant local effects.

\section{Results and discussions}

During the > 500 days measurement period the SST is found to vary between
~ 20\,{\degree}C and ~ 28\,{\degree}C with minimum and maximum
occurring around mid-March and mid-July. (Fig.~10, light blue
curve). Figure~10 shows our corrected records of humidity (green), relative
humidity normalized to SST (red), \chem{\delta^{18}O} (blue), and d-excess
(black) for the period between November~2011 and June~2013 (6\,h data).
Thanks to limited prolonged data gaps our data coverage is 95\,{\%}. The
first gap in the data (~ 2012.25) was due to a~flooded inlet caused by
heavy rain, while the second gap (~ 2012.4) was due to a~failure of
a~vacuum pump.

The full year of data from 2012 allow us to compute the annual mean value for
the humidity, \chem{\delta^{18}O}, δD, and d-excess: $\sim
20$\,500\,\unit{ppmv}, 70\,{\%} (rhSST), $-$11.81\,{\permil},
$-$80.8\,{\permil}, and 13.7\,{\permil}. We find for 2012 a~well-defined
maximum (minimum) for \chem{\delta^{18}O} (d-excess) to occur in July
($-$10.0\,{\permil} and 7.3\,{\permil}), while the months November--February
have roughly similar minimum (maximum) \chem{\delta^{18}O} (d-excess) mean
values ($-$12.5\,{\permil} to $-$12.8\,{\permil} and 16.8\,{\permil} to
17.7\,{\permil}). Figure~10 clearly shows July--August to have less
variability (standard deviation (σ) of the 6\,h data) in
\chem{\delta^{18}O} and d-excess: ~ 1.03\,{\permil} and $\sim
3$\,{\permil} than January--February ($\sigma (\delta ^{18}$O) and $\sigma
$($d$-excess): ~ 1.8\,{\permil} and ~ 9\,{\permil}). We notice the
absence of a~significant diurnal variation in the humidity and isotopes
indicating the absence of local diurnal processes related to the boundary
layer and plant transpiration (Welp et~al., 2012; Berkelhammer et~al., 2013).

From the 6\,hourly data, d-excess is strongly correlated with rhSST
($n=\sim 2100$, $R = -0.93$); with a~slope of $-$42.6\,$\pm$\,0.4\,{\permil}

per {{\%}} (Table~2, Fig.~11a). For the remainder of this section, we further investigate the stability of the relationship between d-excess and rhSST, comparing the results obtained under different wind regimes, and different seasons (based on SST values).

The observed relationships are compared to theoretical calculations based on MJ79 performed for a~smooth surface (wind speed below 6\,\unit{m\,s^{-1}}) and a~rough surface (wind speed above 7\,\unit{m\,s^{-1}} — kinetic fractionation value take for 10\,\unit{m\,s^{-1}}) and for SST of 20\,{\degree}C and 30\,{\degree}C. The best linear fit to our observations is extremely close to MJ79 predictions for a~smooth surface, and bracketed by calculations for SST between 20\,{\degree}C and 30\,{\degree}C. It is also found that the predictions corresponding to a~rough surface and SST of 20\,{\degree}C constitute a~lower bound for the observations.

Note that this comparison relies on the implicit assumption that Tudor Hill winds and relative humidity (measured at about 49\,\unit{m}\,a.s.l.) are representative of meteorological conditions of the lower boundary layer. Based on the similarity of humidity variations (despite a~systematic offset) with the other end of the Bermuda Islands (Fig.~1), and the lack of a~strong diurnal variability, which could be driven by changes in the marine boundary layer height, we assume this implicit hypothesis to be valid.

In order to investigate if the observed relationship depends on the wind regime, Fig.~11b shows the subsets of observations corresponding to wind conditions associated with a smooth surface (wind speed < 6\,\unit{m\,s^{-1}} -- blue dots) and a~rough surface (wind speed > 7\,\unit{m\,s^{-1}} -- red dots). We made the separation according to the discontinuity in the kinetic fractionation factor defined by MJ79. A~small difference between the two subsets appears for rhSST\,< 0.6, with smooth conditions associated with higher ranges of d-excess. The slope of the relationship between d-excess and rhSST is slightly more negative ($-$43\,{\permil} per {{\%}} vs. $-$42\,{\permil} per {{\%}}) for data corresponding to low winds. However, this observed difference is much smaller than inferred from MJ79 (from $-$42.7 to $-$28.5\,{\permil} per {{\%}} when shifting from smooth to rough surface). This indicates that either the wind regimes defined in MJ79 might not be appropriate for this area or the observed d-excess of the local water vapor is affected by past wind conditions at remote areas of evaporation. The differences between the result of this study and the results by Uemura et al.~(2012) and Benetti et al.~(2014) illustrates that more studies are needed to clarify the effect of wind speed on the d-excess signal in the marine boundary layer.

\subsection{Seasonal d-excess vs. rh}

We now investigate whether the relationship between d-excess and rhSST varies as a~function of SST and season. The winter period is defined for SST below 21.0\,{\degree}C, summer for SST above 26.0\,{\degree}C, and spring and autumn for SST between 23.0\,{\degree}C and 25.0\,{\degree}C. Figure~11c and~d show the d-excess vs. rhSST for the different periods as well as the best linear fits (summarized in Table~2). The average rhSST for both the

complete data set and for the winter subset data is approximately 60--65\,{\%}. Comparing for this rhSST the absolute values of the best fit shown in Fig.~11 and in Table~2 reveal the winter d-excess to be about 1\,{\permil} lower compared to that for the complete data set (~ 17\,{\permil} compared to ~ 18\,{\permil}). This offset is consistent with the theory of MJ79 and the dependency of d-excess on SST: 3\,{\degree}C lower winter SST is expected to decrease winter d-excess by approximately 1\,{\permil}. With similar SST and rh ranges, we also observe that d-excess is systematically higher in autumn than in spring, which also translates into different intercepts of d-excess vs. rhSST regressions (Fig.~11d, Table~2). This feature, which cannot be explained by local meteorological parameters (i.e. SST), points to a~change of moisture source region(s) and/or condition between spring and autumn. The validation of this hypothesis requires specific investigations such as moisture back-trajectory calculations, or water tagging using atmospheric general circulation models, which are beyond the scope of this manuscript.

Finally, Fig.~11c and~d and Table~2 highlight that the slope between d-excess and rhSST is much more negative in summer than for other seasons. The distribution of the summer d-excess data shows a~subset of points for rhSST\,> 0.65 which are aligned on the same d-excess vs. rhSST relationship as for the winter season. However, a~subset of abnormal high summer d-excess data corresponding to rhSST\,< 0.65, and dominant northwesterly winds, lead to a~much more negative slope with respect to local rhSST. Section~3.3 will systematically investigate the influence of wind direction on the d-excess.

\subsection{d-excess vs. rh on different time scales}

Figure~10 clearly depicts enhanced winter variability in surface humidity and isotopic composition. This is supported by a~wavelet analysis showing significant power in the variability of the humidity and isotopes with periodicities between 3 to 8 days from mid-November to mid-February. During the summer months (mid-April to mid-September), no period with a~significant power show up. This is consistent with the build-up and westerly shift of the Bermuda-Azores high pressure system during summer. This prevents frontal systems from passing through the area compared to the winter period when the high pressure system is weaker and frontal systems are able to move across Bermuda (Huang et~al., 1999; Portis et~al., 2001). As different weather systems dominate the isotopic variability during different seasons, we used a wavelet coherence analysis to characterize the relationship between d-excess and rh in the frequency and time domain (not shown). It confirms that d-excess and rh time series are strongly anti-correlated over the full data period on time scales between ~ 1--2 days and up to 2 months (the length of dataset does not allow this analysis to be extended on longer time scales). The lack in correlation on time scale below 1--2 days may be due to the analytical limitation, and the too low signal-to-noise ratio of our d-excess measurements.

Due to the strong anti-correlation between d-excess and rhSST on time scales of days to months, it is possible to investigate the relation between d-excess and rhSST for different averaging time scales. We divide the record into separate non-overlapping periods ranging from one day and up to one month. The estimated slope of the daily to monthly averaged d-excess vs. rhSST values is shown in Fig.~12 as function of the averaging period. We

find that the slope for d-excess vs. rhSST changes from $\sim$ $-43.6\,$\$\pm\$$\,0.7$ ($R^2=0.86$, $n=494$) to $\sim$ $-52.0\,$\$\pm\$$\,3.3\,$\{\permil} per {{\%}} ($R^2=0.86$, $n=36$) when increasing the averaging time from 1 day to 2 weeks. Increasing the averaging time from 2-weeks to 1 month does not significantly further affect this slope further. We note that time averaging allows for integration across synoptic systems. This is comparable to a spatial averaging across air masses in the region around the Bermuda Islands. While the daily slope is consistent with that of MJ79, increasing averaging time causes the slope to deviate from the theoretical slope of MJ79 and to become closer to the value found by Uemura et~al.~(2008) from their transect across the Southern Ocean. As the theoretical slope of MJ79 is based on the closure assumption, we hypothesize that the deviation from this slope with increased averaging time (averaging across synoptic systems) reflect that this assumption is no longer valid. Further studies are required to support this speculation. Future comparisons between observations and results from atmospheric general circulation models should clearly include the analysis of the relationship between d-excess and rhSST along different frequencies, as shown in Fig.~12.

\subsection{Influence of wind direction on d-excess}

In previous sections, we have reported several findings, which suggest that changes in moisture advection (and moisture sources) might affect the variability of the d-excess measured in Bermuda. Figure~13 depicts the distribution of d-excess (contours) as a~function of relative humidity (x-axis) and wind direction (y-axis), for summer (upper panel) and winter (lower panel), and the differences in relationships between d-excess and rhSST for subsets based on specific sectors (subjectively defined) of wind direction. In summer, we find that the d-excess vs. rhSST obtained during wind from the western sector has a~very negative slope of $-$56.7\,$\pm\,2.2\,$\{\permil} per {{\%}}. We conclude that westerly winds cause high summer d-excess levels, possibly due to high kinetic effect induced by warm, dry air masses coming off the American continent (Pfahl and Sodemann, 2013; Gat et~al., 2003). In winter, differences in slopes are also identified for specific wind sectors, the southwestern sector (wind directions 200--250{\degree}) leading to the most negative slope and the highest d-excess levels for a~given rhSST (Table~2). The dependency of the slope of d-excess vs. rhSST against wind direction illustrates the limitation of the closure assumption and the need for long-term monitoring in order to deduce the drivers of the d-excess in the marine boundary layer.

\conclusions

In order to monitor the drivers of marine boundary layer d-excess of the subtropical North Atlantic, we have presented continuous long-term observations of surface water vapor isotopic composition over a~$\sim$ 1.5\,\unit{yr} period between November~2011 and June~2013 from the Bermuda Islands. Thanks to meticulous independent calibration protocols, the inter-comparison of two parallel analyzers shows that the accuracy and precision of 10\,min averages of \chem{\delta^{18}O}, δD, and d-excess is 0.14\,{\permil}, 0.85\,{\permil}, and 1.1\,{\permil}. Tests on our monitoring system show that isotopic signals can be accurately retrieved with a~temporal resolution down to 1\,min intervals. During a~few days, parallel measurements recorded by separated water vapor isotope analyzers on each end of the Bermuda Islands show a~common signal

within these 20\,\unit{km}, suggesting a limited effect of the island. We
conclude that the signal is dominated by the marine boundary layer moisture.

The accuracy and precision of the d-excess measurements allow us to
document and investigate the controls on the d-excess variability. In
accordance with theory, d-excess variability is driven by the relative
humidity of the air normalized to sea surface temperature. However, we could
not identify any shifts in relationship with wind speed. In Bermuda, the
relationship between d-excess and relative humidity depends on the season,
and thereby SST. Moreover, specific wind directions (western winds in summer,
and southwestern winds in winter) lead to unusually high d-excess values
for a~given humidity level, and a~higher negative slope between d-excess
and humidity. This feature stresses the limitation of the closure assumption
and calls for long-term monitoring in order to characterize the complete set
of processes controlling the variability of surface moisture d-excess. Such
long-term monitoring indeed allows to evidence processes other than relative
humidity (e.g. SST, wind direction{\ldots}), which act on d-excess. We have
clearly demonstrated the change of d-excess vs. relative humidity slope as
a~function of the averaging period (from 1 day to 2 months). Extending our
record in time will allow for the investigation of the drivers of d-excess
at the inter-annual scale. A~next step will be to diagnose changes in
moisture source and remote evaporation conditions, using back trajectory
calculations and water tagging within atmospheric models in order to take
into account the advection effects highlighted by the impact of wind
directions. Our dataset will in the future be used to test the validity of
deuterium retrievals based on remote sensing (Lacour et~al.,~2012), and to
benchmark atmospheric general circulation models equipped with water stable
isotopes (Werner et~al., 2011; Risi et~al., 2010; Yoshimura et~al., 2008).

\begin{thebibliography}{99}

\bibitem{1}
Acker,~J.~G. and Leptoukh,~G.: Online analysis enhances use of nasa earth
science data, EOS T. Am. Geophys. Un., 88, 14--17, \doi{10.1029/2007eo020003},
2007.

\bibitem{2}
Baer,~D.~S., Paul,~J.~B., Gupta,~M., and O'Keefe,~A.: Sensitive absorption
measurements in the near-infrared region using off-axis integrated-cavity-output

spectroscopy, Appl. Phys. B-Lasers O., 75, 261--265, \doi{10.1007/s00340-002-0971-z}, 2002.

\bibitem{3}
Bastrikov, V., Steen-Larsen, H. C., Masson-Delmotte, V., Gribanov, K., Cattani, O., Jouzel, J., and Zakharov, V.: Continuous measurements of atmospheric water vapour isotopes in Western Siberia (Kourovka), Atmos. Meas. Tech. Discuss., 7, 475--507, doi:10.5194/amtd-7-475-2014, 2014.

\bibitem{4}
Benetti,~M., Reverdin,~G., Pierre,~C., Merlivat,~L., Risi,~C., Steen-Larsen,~H.~C., and Vimeux,~F.: Deuterium excess in marine water vapor: dependency on relative humidity and surface wind speed during evaporation, J. Geophys. Res.-Atmos., 119, 584-593, doi:10.1002/2013JD020535, ~2014.

\bibitem{5}
Bonne,~J.-L., Masson-Delmotte,~V., Cattani,~O., Delmotte,~M., Risi,~C., Sodemann,~H., and Steen-Larsen,~H.~C.: The isotopic composition of water vapour and precipitation in Ivittuut, Southern Greenland, Atmos. Chem. Phys. Discuss., 13, 30521--30574, \doi{10.5194/acpd-13-30521-2013}, 2013.

\bibitem{6}
Berkelhammer,~M., Hu,~J., Bailey,~A., Noone,~D.~C., Still,~C.~J., Barnard,~H., Gochis,~D., Hsiao,~G.~S., Rahn,~T., and Turnipseed,~A.: The nocturnal water cycle in an open-canopy forest, J. Geophys. Res.-Atmos., 118, 10225--10242, \doi{10.1002/jgrd.50701}, 2013.

\bibitem{7}
Brutsaert,~W.: A~theory for local evaporation (or heat transfer) from rough and smooth surfaces at ground level, Water Resour. Res., 11, 543--550, \doi{10.1029/WR011i004p00543}, 1975.

\bibitem{8}
Craig,~H.: Standard for reporting concentrations of deuterium and oxygen-18 in natural waters, Science, 133, 1833--1834, \doi{10.1126/science.133.3467.1833}, 1961a.

\bibitem{9}
Craig,~H.: Isotopic variations in meteoric waters, Science, 133, 1702--1703, 1961b.

\bibitem{10}
Craig,~H. and Gordon,~L.~I.: Deuterium and oxygen 18 variations in the ocean and the marine atmosphere, in: Stable Isotopes in Oceanographic Studies and Paleotemperatures, 26--30 July~1965, Spoleto, Italy, 1965.

\bibitem{11}
Crosson,~E.~R., Ricci,~K.~N., Richman,~B.~A., Chilese,~F.~C., Owano,~T.~G., Provencal,~R.~A., Todd,~M.~W., Glasser,~J., Kachanov,~A.~A., Paldus,~B.~A., Spence,~T.~G., and Zare,~R.~N.: Stable isotope ratios using cavity ring-down spectroscopy: determination of C-13/C-12 for carbon dioxide in human breath, Anal. Chem., 74, 2003--2007, \doi{10.1021/ac025511d}, 2002.

\bibitem{12}

Dansgaard,~W.: The O^{18}-abundance in fresh water, Geochim. Cosmochim. Ac., 6, 241--260, 1954.

\bibitem{13}
Dansgaard,~W.: Stable isotopes in precipitation, Tellus, 16, 436--468, 1964.

\bibitem{14}
Ellehoj,~M.~D., Steen-Larsen,~H.~C., Johnsen,~S.~J., and Madsen,~M.~B.: Ice-vapor equilibrium fractionation factor of hydrogen and oxygen isotopes: Experimental investigations and implications for stable water isotope studies, Rapid Commun. Mass Sp., 27, 2149--2158, \doi{10.1002/rcm.6668}, 2013.

\bibitem{15}
Epstein,~S. and Mayeda,~T.: Variation of the 18-o content of waters from natural sources, Geochim. Cosmochim. Ac., 4, 213--224, 1953.

\bibitem{16}
Fisher,~D.~A.: Stable isotope simulations using a~regional stable isotope model coupled to a~zonally averaged global model, Cold Reg. Sci. Technol., 21, 61--77, 1992.

\bibitem{17}
Gat,~J.~R., Klein,~B., Kushnir,~Y., Roether,~W., Wernli,~H., Yam,~R., and Shemesh,~A.: Isotope composition of air moisture over the mediterranean sea: an index of the air--sea interaction pattern, Tellus B, 55, 953--965, 2003.

\bibitem{18}
Haines,~S.~L., Jedlovec,~G.~J., and Lazarus,~S.~M.: A~modis sea surface temperature composite for regional applications, IEEE T. Geosci. Remote, 45, 2919--2927, \doi{10.1109/tgrs.2007.898274}, 2007.

\bibitem{19}
Huang,~S., Rahn,~K.~A., Arimoto,~R., Graustein,~W.~C., and Turekian,~K.~K.: Semiannual cycles of pollution at bermuda, J. Geophys. Res.-Atmos., 104, 30309--30317, \doi{10.1029/1999jd900801}, 1999.

\bibitem{20}
Johnsen,~S.~J.: Stable isotope homogenization of polar firn and ice. Proc. of Symp. on Isotopes and Impurities in Snow and Ice, i.~U.~G.~G. XVI, general assembly, Grenoble, August--September 1975, IAHS-AISH P., 118, 210--219, 1977.

\bibitem{21}
Johnsen,~S.~J., Dansgaard,~W., and White,~J.~W.~C.: The origin of arctic precipitation under present and glacial conditions, Tellus B, 41, 452--468, 1989.

\bibitem{22}
Johnsen,~S.~J., Clausen,~H.~B., Cuffey,~K.~M., Hoffmann,~G., Schwander,~J., and Creyts,~T.: Diffusion of stable isotopes in polar firn and ice: the isotope effect in firn diffusion, in: Physics of Ice Core Records, edited by: Hondoh,~T., Hokkaido University Press, Sapporo, 121--140, 2000.

\bibitem{23}
Jouzel,~J., Alley,~R.~B., Cuffey,~K.~M., Dansgaard,~W., Grootes,~P., Hoffmann,~G., Johnsen,~S.~J., Koster,~R.~D., Peel,~D., Shuman,~C.~A.,

Stievenard,~M., Stuiver,~M., and White,~J.: Validity of the temperature reconstruction from water isotopes in ice cores, J. Geophys. Res., 102, 26471--26487, 1997.

\bibitem{23a}
Jouzel,~J., Sti\'{e}venard,~M., Johnsen,~S.~J., Landais,~A., Masson-Delmotte,~V., Sveinbjornsdottir,~A., Vimeux,~F., von Grafenstein,~U., and White,~J.~W.~C.: The GRIP deuterium-excess record, Quaternary Sci. Rev., 26, 1--17, \doi{10.1016/j.quascirev.2006.07.015}, 2007.

\bibitem{24}
Kurita,~N.: Origin of arctic water vapor during the ice-growth season, Geophys. Res. Lett., 38, L02709, \doi{10.1029/2010gl046064}, 2011.

\bibitem{25}
Lacour,~J.-L., Risi,~C., Clarisse,~L., Bony,~S., Hurtmans,~D., Clerbaux,~C., and Coheur,~P.-F.: Mid-tropospheric δD observations from IASI/MetOp at high spatial and temporal resolution, Atmos. Chem. Phys., 12, 10817--10832, \doi{10.5194/acp-12-10817-2012}, 2012.

\bibitem{26}
Majoube,~M.: Fractionnement en oxyg\`{e}ne 18 et en deut\'{e}rium entre l'eau et sa vapeur,~J. Climate Phys., 68, 1423--1436, 1971.

\bibitem{27}
Massman,~W.~J. and Ibrom,~A.: Attenuation of concentration fluctuations of water vapor and other trace gases in turbulent tube flow, Atmos. Chem. Phys., 8, 6245--6259, \doi{10.5194/acp-8-6245-2008}, 2008.

\bibitem{28}
Masson-Delmotte,~V., Landais,~A., Stievenard,~M., Cattani,~O., Falourd,~S., Jouzel,~J., Johnsen,~S.~J., Dahl-Jensen,~D., Sveinbjornsdottir,~A., White,~J.~W.~C., Popp,~T., and Fisher,~H.: Holocene climatic changes in greenland: different deuterium excess signals at greenland ice core project (grip) and northgrip, J. Geophys. Res., 110, D14102, \doi{10.1029/12004JD005575}, 2005.

\bibitem{29}
Merlivat,~L. and Jouzel,~J.: Global climatic interpretation of the deuterium-oxygen 18 relationship for precipitation, J. Geophys. Res., 84, 5029--5033, 1979.

\bibitem{30}
Pfahl,~S. and Sodemann,~H.: What controls deuterium excess in global precipitation?, Clim. Past Discuss., 9, 4745--4770, \doi{10.5194/cpd-9-4745-2013}, 2013.

\bibitem{31}
Pfahl,~S.~and Wernli,~H.: Lagrangian simulations of stable isotopes in water vapor -- an evaluation of non-equilibrium fractionation in the Craig--Gordon model,~J.~Geophys. Res., 114, D20108,~\doi{10.1029/2009JD012054}, 2009

\bibitem{32}
Portis,~D.~H., Walsh,~J.~E., El Hamly,~M., and Lamb,~P.~J.: Seasonality of the north atlantic oscillation, J. Climate, 14, 2069--2078,

\doi{10.1175/1520-0442(2001)012.0.CO;2}, 2001.

\bibitem{33}
Risi,~C., Bony,~S., Vimeux,~F., and Jouzel,~J.: Water stable isotopes in the
lmdz4 general circulation model: model evaluation for present day and past
climates and applications to climatic interpretations of tropical isotopic
records, J. Geophys. Res., 115, D12118, \doi{10.1029/2009JD013255}, 2010.

\bibitem{34}
Rozanski,~K., Aragu\'{a}s-Aragu\'{a}s,~L., and Gonfiantini,~R.: Isotopic
patterns in modern global precipitation, in: Climate Change in Continental
Isotopic Records, Geophys.~Monogr. Ser. Vol. 78, American Geophysical Union
(AGU), Washington,~DC, 1--36, 1993.

\bibitem{35}
Spank,~U. and Bernhofer,~C.: Another simple method of spectral correction to
obtain robust Eddy-covariance, Bound.-Lay. Meteorol., 128, 403--422,
\doi{10.1007/s10546-008-9295-9}, 2008.

\bibitem{36}
Steen-Larsen,~H.~C., Masson-Delmotte,~V., Sjolte,~J., Johnsen,~S.~J.,
Vinther,~B.~M., Breon,~F.~M., Clausen,~H.~B., Dahl-Jensen,~D., Falourd,~S.,
Fettweis,~X., Gallee,~H., Jouzel,~J., Kageyama,~M., Lerche,~H., Minster,~B.,
Picard,~G., Punge,~H.~J., Risi,~C., Salas,~D., Schwander,~J., Steffen,~K.,
Sveinbjornsdottir,~A.~E., Svensson,~A., and White,~J.: Understanding the
climatic signal in the water stable isotope records from the neem shallow
firn/ice cores in northwest greenland, J. Geophys. Res.-Atmos., 116, D06108,
\doi{10.1029/2010jd014311}, 2011.

\bibitem{37}
Steen-Larsen,~H.~C., Johnsen,~S.~J., Masson-Delmotte,~V., Stenni,~B.,
Risi,~C., Sodemann,~H., Balslev-Clausen,~D., Blunier,~T., Dahl-Jensen,~D.,
Elleh{\o}j,~M.~D., Falourd,~S., Grindsted,~A., Gkinis,~V., Jouzel,~J.,
Popp,~T., Sheldon,~S., Simonsen,~S.~B., Sjolte,~J., Steffensen,~J.~P.,
Sperlich,~P., Sveinbj\"{o}rnsd\'{o}ttir,~A.~E., Vinther,~B.~M., and
White,~J.~W.~C.: Continuous monitoring of summer surface water vapor isotopic
composition above the Greenland Ice Sheet, Atmos. Chem. Phys., 13,
4815--4828, \doi{10.5194/acp-13-4815-2013}, 2013.

\bibitem{38}
Tremoy,~G., Vimeux,~F., Mayaki,~S., Souley,~I., Cattani,~O., Risi,~C.,
Favreau,~G., and Oi,~M.: A~1\,yr long \chem{\delta^{18}O} record of water vapor
in Niamey (Niger) reveals insightful atmospheric processes at different
timescales,~Geophys. Res. Lett.,~39, L08805, \doi{10.1029/2012GL051298}, 2012.

\bibitem{39}
Uemura,~R., Matsui,~Y., Yoshimura,~K., Motoyama,~H., and Yoshida,~N.: Evidence
of deuterium excess in water vapor as an indicator of ocean surface conditions,
J. Geophys. Res.-Atmos., 113, D19114, \doi{10.1029/2008jd010209}, 2008.

\bibitem{40}
Welp,~L.~R., Lee,~X., Griffis,~T.~J., Wen,~X.-F., Xiao,~W., Li,~S., Sun,~X.,
Hu,~Z., Val Martin,~M., and Huang,~J.: A~meta-analysis of water vapor deuterium-
excess in the midlatitude atmospheric surface layer, Global Biogeochem. Cy., 26,
GB3021, \doi{10.1029/2011gb004246}, 2012.

\bibitem{41}
Werner,~M., Langebroek,~P.~M., Carlsen,~T., Herold,~M., and Lohmann,~G.: Stable
water isotopes in the echam5 general circulation model: toward high-resolution
isotope modeling on a~global scale, J. Geophys. Res.-Atmos., 116, D15109,
\doi{10.1029/2011jd015681}, 2011.

\bibitem{42}
Yoshimura,~K., Kanamitsu,~M., Noone,~D., and Oki,~T.: Historical isotope
simulation using reanalysis atmospheric data, J. Geophys. Res.-Atmos., 113,
D19108, \doi{10.1029/2008jd010074}, 2008.

\end{thebibliography}

\begin{table}%T1
\caption{Slope between IAEA VSMOW-SLAP values and measured values of standards.}
\begin{tabular}{lccccccccc}
  \tophline
  Date&\multicolumn{2}{c}{Slope} &\multicolumn{2}{c}{Standard}
&\multicolumn{2}{c}{Mean slope} &\multicolumn{2}{c}{Standard} \\
  & & &\multicolumn{2}{c}{deviation slope} & & &\multicolumn{2}{c}{deviation
mean} \\
  & & &\multicolumn{2}{c}{~} & & &\multicolumn{2}{c}{slope} \\
  &\chem{\delta^{18}O}&δD&\chem{\delta^{18}O}&$\delta
D$&\chem{\delta^{18}O}&$\delta D$&\chem{\delta^{18}O}&$\delta D$ \\
  \middlehline
  27~Nov~2011&1.0708&1.0685&0.0206&0.0104&--&--&--&-- \\
   \middlehline
  28~Aug~2012&1.0713&1.0915&0.0029&0.0055&1.0733&1.09315&0.0052&0.0078 \\
  31~Aug~2012&1.0756&1.0886&0.0062&0.0047&&&&\\
  4~Sep~2012&1.0690&1.0949&0.0033&0.0033&&&&\\
  6~Sep~2012&1.0812&1.1081&0.0203&0.0051&&&&\\
  10~Sep~2012&1.0756&1.0883&0.0023&0.0100&&&&\\
  15~Sep~2012&1.0669&1.0875&0.0026&0.0064&&&&\\ \middlehline
  13~Jun~2013&1.0527&1.0759&0.0044&0.0049&1.0547&1.0756&0.0022&0.0003 \\
  2~Jul~2013&1.0571&1.0753&0.0014&0.0024&&&&\\
  3~Jul~2013&1.0543&1.0755&--&--&&&&\\
  \bottomhline
\end{tabular}
\label{tab1}
\end{table}

\begin{table}%T2
\caption{The slope and intersect of d-excess vs. relative humidity for the
complete data set as well as seasonal, wind direction, and wind speed
subsets.}
\begin{tabular}{llcccc}
\tophline
&&Slope&Intercept&R^2&N \\

```
&& [{\permil}\,[rh$^{-1}$]]& [{\permil}]&& \\
\middlehline
All data&&$-$42.6\,$\pm$\,0.4&43.5\,$\pm$\,0.3&0.86&1926 \\
&High wind speed ($> 7$\,\unit{m\,s^{-1}})&$-$
$42.0\,$\pm$\,0.5&42.9\,$\pm$\,0.4&0.89&679 \\
&Low wind speed ($< 6$\,\unit{m\,s^{-1}})&$-$
$43.0\,$\pm$\,0.6&43.9\,$\pm$\,0.4&0.82&1016 \\
\cline{1-6}
Summer data&&$-$51.9\,$\pm$\,1.5&50.8\,$\pm$\,1.1&0.76&398 \\
&Wind direction 0--180{\degree} &$-$45.2\,$\pm$\,2.1&46.3\,$\pm$\,1.5&0.69&208
\\
&Wind direction 180--360{\degree} &$-$56.7\,$\pm$\,2.1&54.1\,$\pm$\,1.6&0.80&180
\\
\cline{1-6}
Winter data&&$-$40.7\,$\pm$\,0.5&41.4\,$\pm$\,0.4&0.88&738 \\
&Wind direction 0--200{\degree} &$-$41.7\,$\pm$\,0.8&42.5\,$\pm$\,0.6&0.88&287
\\
&Wind direction 200--250{\degree} &$-$49.1\,$\pm$\,1.0&48.6\,$\pm$\,0.8&0.92&164
\\
&Wind direction 250--360{\degree} &$-$38.7\,$\pm$\,1.1&39.8\,$\pm$\,0.6&0.82&275
\\
\cline{1-6}
Autumn data&&$-$37.4\,$\pm$\,1.1&41.8\,$\pm$\,0.7&0.90&135 \\
\cline{1-6}
Spring data&&$-$39.1\,$\pm$\,1.8&40.0\,$\pm$\,1.4&0.85&90 \\
\bottomhline
\end{tabular}
\label{tab2}
\end{table}


\begin{figure}
\includegraphics[width=120mm]{acpd-2013-0970-f01}
\caption{Illustration of the position of the Bermuda Islands
  \textbf{(A)}, map of the sites where observations have been
  performed at Tudor Hill Atmospheric Observatory and on the other
  site of the island \textbf{(B)}, system setup \textbf{(C)}. The wind
  rose (6\,hourly observations) indicates that the wind is
  predominantly arriving to Tudor Hill directly from the ocean
  \textbf{(D)}.}
\label{acpd-2013-0970-f01}
\end{figure}

\begin{figure}
\includegraphics[width=40mm]{acpd-2013-0970-f02}
\caption{Humidity-isotope response calibrations of the analyzer
  performed at different dates during the monitoring period. The lower
  panel represents the best fit using either a~second or third order
  polynomial to the observations.}
\label{acpd-2013-0970-f02}
\end{figure}

\begin{figure}
\includegraphics[width=55mm]{acpd-2013-0970-f03}
```

```
\caption{Drift on the measured isotopic values. The top panel shows
  the temperature of the water body in the bubbler system. Below is
  shown the internal temperature of the Picarro analyzer (DAS
  temperature). The theoretical drift of the calibration water vapor
  isotopes is calculated, based on the drift of the calibration
  temperature. The observed drift in \chem{\delta^{18}O}, $\delta D$,
  and $d$-excess is shown for individual measurements in blue, red,
  and green dots. The 48\,h running mean is shown using a~black solid
  line.}
\label{acpd-2013-0970-f03}
\end{figure}

\begin{figure}
\includegraphics[width=90mm]{acpd-2013-0970-f04}
\caption{Relationship between the observed absolute humidity by the
  Campbell humidity sensor (y-axis) and the measurement by the Picarro
  analyzer (x-axis). This relationship is used to correct the Picarro
  humidity measurements.}
\label{acpd-2013-0970-f04}
\end{figure}

\begin{figure}
\includegraphics[width=100mm]{acpd-2013-0970-f05}
\caption{Results of experiments conducted to characterize the response
  time of the system. Step changes of humidity followed by step
  changes in \chem{\delta^{18}O} were performed. Note that the steps
  are not of equal length as the experiment was performed on an ad-hoc
  field setup on top of the tower.}
\label{acpd-2013-0970-f05}
\end{figure}

\begin{figure}
\includegraphics[width=120mm]{acpd-2013-0970-f06}
\caption{Normalized response function for humidity,
  \chem{\delta^{18}O}, and $\delta D$ (upper panel). Time-derivative
  of the normalized response functions (lower panel).}
\label{acpd-2013-0970-f06}
\end{figure}

\begin{figure}
\includegraphics[width=120mm]{acpd-2013-0970-f07}
\caption{Fourier transform of the time-derivative normalized response
  functions for humidity, \chem{\delta^{18}O}, and $\delta D$. The
  transfer functions of the humidity and isotopes are estimated for
  each of the 3 steps shown in Fig.~5.}
\label{acpd-2013-0970-f07}
\end{figure}

\begin{figure}
\includegraphics[width=90mm]{acpd-2013-0970-f08}
\caption{Observed humidity, \chem{\delta^{18}O}, and $d$-excess by
  two independently calibrated water vapor isotope analyzers installed
  in parallel using the same inlet on the tower. The observations are
  reported as 10\,min averages. The estimated uncertainties for
  \chem{\delta^{18}O} and $d$-excess based on the standard deviation
```

```
  of the inter-instrument anomaly (0.14\,{\permil} and 1.1\,{\permil})
  are indicated next to the axes.}
\label{acpd-2013-0970-f08}
\end{figure}

\begin{figure}
\includegraphics[width=60mm]{acpd-2013-0970-f09}
\caption{Humidity, \chem{\delta^{18}O}, and $d$-excess measured by
  two water vapor analyzers separated to opposite ends of the
  island. We highlight an event where an increase in humidity and
  \chem{\delta^{18}O} is first recorded at the northern site and 1\,h
  later at Tudor hill as expected by surface wind direction and wind
  speed during this period. The estimated uncertainties for
  \chem{\delta^{18}O} and $d$-excess (0.14\,{\permil} and
  1.1\,{\permil}) are indicated next to the axes.}
\label{acpd-2013-0970-f09}
\end{figure}

\begin{figure}
\includegraphics[width=120mm]{acpd-2013-0970-f10}
\caption{SST, humidity and water vapor isotopic composition monitored
  between November 2011 and June 2013. From top to bottom are shown
  the sea surface temperature [{\degree}C] (cyan), humidity [ppmv]
  (green), the relative humidity normalized to sea surface temperature
  (red), the water vapor \chem{\delta^{18}O} [{\permil}] (blue) and
  $d$-excess [{\permil}] (black).}
\label{acpd-2013-0970-f10}
\end{figure}

\begin{figure}
\includegraphics[width=90mm]{acpd-2013-0970-f11}
\caption{\textbf{(A)} Complete set of 6\,hourly observations of
  $d$-excess vs. relative humidity (rhSST) at sea surface
  temperature (black dots), with a~best fit (grey line). Results from
  the theory of MJ79 are displayed for a~rough and smooth
  surface, and for SST of 20\,{\degree}C and
  30\,{\degree}C. \textbf{(B)} The complete set of 6\,hourly
  observations of $d$-excess vs. rhSST separated into calm ($<
  6$\,\unit{m\,s^{-1}} -- cyan dots) and strong winds ($>
  7$\,\unit{m\,s^{-1}} -- grey dots). MJ79 calculations are shown for
  a~rough and smooth surface at 20\,{\degree}C. \textbf{(C)}
  Observations collected during winter (defined as SST\,$<
  21$\,{\degree}C -- blue dots) and summer (defined as SST\,$>
  26$\,{\degree}C -- red dots) period. The best linear fits to winter
  and summer observations are shown as respectively black and grey
  solid lines. \textbf{(D)} Observations collected during spring
  (23\,{\degree}C\,$<$\,SST\,$< 25$\,{\degree}C -- green dots) and autumn
  (23\,{\degree}C\,$<$\,SST\,$< 25$\,{\degree}C -- brown dots) period. Best
  linear fits to respectively the spring and autumn period are shown
  as green and brown solid lines.}
\label{acpd-2013-0970-f11}
\end{figure}


\begin{figure}
```

```
\includegraphics[width=120mm]{acpd-2013-0970-f12}
\caption{Slope of $d$-excess vs. RH for different averaging periods
  varying from 1 day to 30\,days.}
\label{acpd-2013-0970-f12}
\end{figure}

\begin{figure}
\includegraphics[width=100mm]{acpd-2013-0970-f13}
\caption{$d$-excess as function of wind direction and relative
  humidity for summer period (SST\,$> 26$\,{\degree}C) (upper panel)
  and for winter period (SST\,$< 21$\,{\degree}C) (lower panel).}
\label{acpd-2013-0970-f13}
\end{figure}

\end{document}
```